N- and C-Terminal Motifs in Human αB Crystallin Play an Important Role in the Recognition, Selection, and Solubilization of Substrates †

ARTICLE *in* BIOCHEMISTRY · DECEMBER 2006

Impact Factor: 3.02 · DOI: 10.1021/bi061471m · Source: PubMed

3 AUTHORS, INCLUDING:

John I Clark
University of Washington Seattle
159 PUBLICATIONS **4,691** CITATIONS

SEE PROFILE

N- and C-Terminal Motifs in Human αB Crystallin Play an Important Role in the Recognition, Selection, and Solubilization of Substrates†

Joy G. Ghosh,‡,§ Ananth K. Shenoy, Jr.,§ and John I. Clark*,‡,§,||

Biomolecular Structure and Design, Department of Biological Structure, and Department of Ophthalmology, University of Washington, Seattle, Washington 98195-7420

Received July 20, 2006; Revised Manuscript Received September 12, 2006

ABSTRACT: The functions of the interactive sequences in human αB crystallin that are involved in chaperone activity and complex assembly of small heat shock proteins need to be characterized to understand the mechanisms of action on unfolding and misfolding proteins. Protein pin arrays identified the hydrophobic N-terminal sequence ($_{41}$STSLSPFYLRPPSFLRAP$_{58}$) and the polar C-terminal sequence ($_{155}$PERTIPITREE$_{165}$) as interactive domains in human αB crystallin, which were then deleted to evaluate their importance in complex assembly and chaperone activity. Size exclusion chromatography determined that the complexes formed by the deletion mutants, Δ41−58 and Δ155−165, were larger and more polydisperse than the wild-type (wt) αB crystallin complex. In chaperone assays, the Δ41−58 mutant was as effective as wt αB crystallin in protecting partially unfolded β_L crystallin and alcohol dehydrogenase (ADH) and significantly less effective than wt αB crystallin in protecting unfolded citrate synthase (CS) from aggregation. Chaperone activity did not correlate with complex size but corresponded with the amount of substrate protein unfolding. The results confirmed the importance of N-terminal residues 41−58 in selective interactions with completely unfolded substrates. Poor solubility and limited or no chaperone activity for the three substrates characterized the Δ155−165 deletion mutant, which demonstrated the importance of C-terminal residues 155−165 in maintaining the solubility of unfolded substrates in a manner independent of the amount of substrate protein unfolding. The results presented in this report established that interactive domains in the N- and C-termini of human αB crystallin are important for the recognition, selection, and solubility of unfolding substrate proteins.

Small heat shock proteins (sHSPs)[1] are a superfamily of low-molecular mass (<43 kDa) stress response proteins that function as molecular chaperones *in vivo* (*1*−*3*). Recent studies used protein pin arrays, mutagenesis, yeast two-hybrid screens, and mass spectrometry to identify interactive sequences in sHSPs (*4*−*11*). Structural studies determined that these interactive sequences were on the surface of the α crystallin core domain of *Methanococcus jannaschii* sHSP 16.5, wheat sHSP16.9, and *Taenia saginata* Tsp36 (*12*−*15*). Systematic biochemical and biophysical characterization of the α crystallin core domain interactive sequences established that the β3−β8−β9 interface on the surface of the α crystallin core domain is important for interactions between sHSPs and unfolded substrate proteins (*16*−*18*). Current research indicates that under conditions of cell stress, sHSPs function through a dynamic equilibrium between a complex of assembled subunits and a pool of activated monomers that bind proteins at the early stages of unfolding (*19*−*27*) to shift the equilibrium from the assembly of sHSP complexes to an assembly of sHSP subunits bound to unfolding/misfolding substrate proteins (*28*−*30*). Sequences that mediate both complex assembly and chaperone activity were previously identified in the N- and C-terminal domains of sHSPs (*7*, *9*−*11*, *31*−*41*). However, the exact role of these N- and C-terminal sequences in the assembly and chaperone activity of sHSPs remains undetermined. The maintenance of unfolded/misfolded protein solubility by molecular chaperones requires recognition of unfolding and misfolding domains on substrate proteins. While chaperone interfaces in sHSPs have been characterized recently, interactive domains in sHSPs responsible for the recognition of unfolded−misfolded proteins are not well characterized. The goal of our studies is to characterize the interactive domains in sHSPs that are responsible for the recognition and selection of unfolding proteins during the cell stress response.

In this report, a systematic study of the hydrophobic interactive sequence ($_{41}$STSLSPFYLRPPSFLRAP$_{58}$) in the N-terminal domain and the polar interactive sequence ($_{155}$PERTIPITREE$_{165}$) in the C-terminal domain of αB crystallin was undertaken to evaluate their contribution to complex assembly and chaperone activity (recognition, selection, binding, and solubility of unfolding substrates). Chaperone assays and size exclusion chromatography determined that N-terminal residues 41−58 are important for complex

† Supported by Grant EY04542 from the National Eye Institute.

* To whom correspondence should be addressed: Department of Biological Structure, HSB G514, Box 357420, University of Washington, Seattle, WA 98195-7420. E-mail: clarkji@u.washington.edu. Phone: (206) 685-0950. Fax: (206) 543-1524.

‡ Biomolecular Structure and Design.

§ Department of Biological Structure.

|| Department of Ophthalmology.

[1] Abbreviations: sHSP, small heat shock protein; UVCD, ultraviolet circular dichroism; ADH, alcohol dehydrogenase; CS, citrate synthase.

10.1021/bi061471m CCC: $33.50
Published on Web 10/31/2006

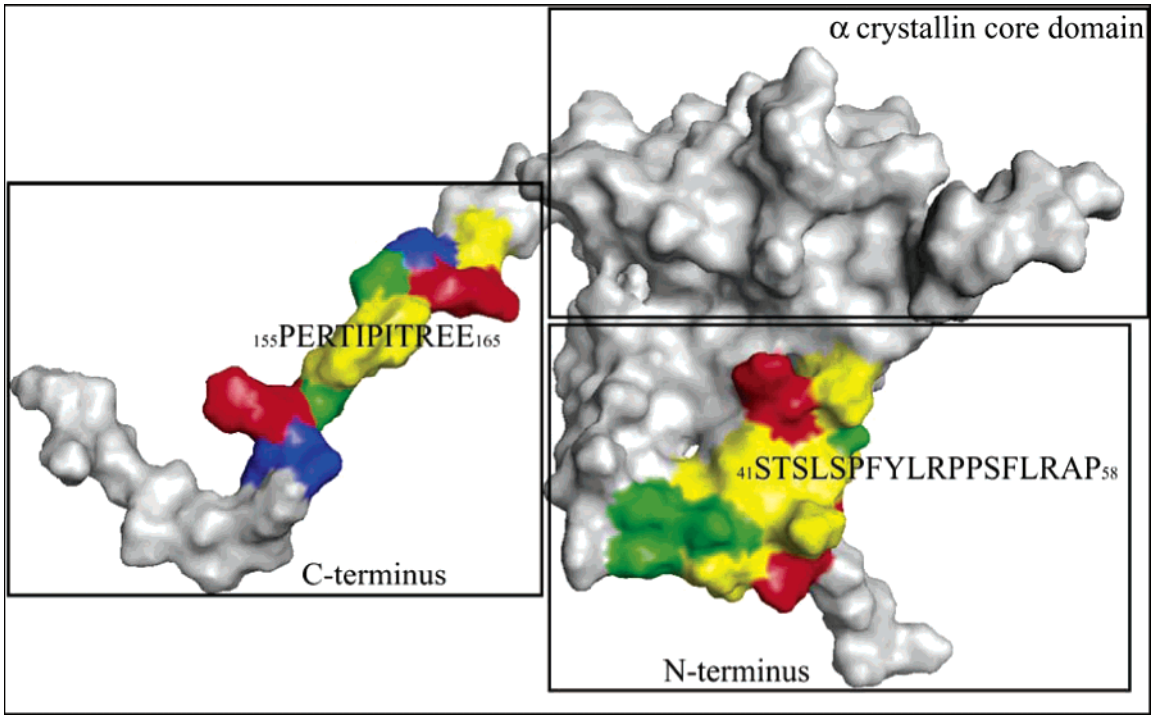

FIGURE 1: 3D model of human αB crystallin. Residues of the N-terminal sequence ($_{41}$STSLSPFYLRPPSFLRAP$_{58}$) and the C-terminal sequence ($_{155}$PERTIPITREE$_{165}$) of human αB crystallin were mapped onto a surface-rendered 3D computed model of human αB crystallin (*9*, *10*). Residues are colored as follows: red for Arg and Lys, blue for Asp and Glu, yellow for Leu, Pro, Phe, Tyr, and Ala, and green for Ser and Thr. The N-terminal sequence ($_{41}$STSLSPFYLRPPSFLRAP$_{58}$) is helical and contains 11 hydrophobic residues (Leu-44, Pro-46, Phe-47, Tyr-48, Leu-49, Pro-51, Pro-52, Phe-54, Leu-55, Ala-57, and Pro-58), two positively charged residues (Arg-50 and Arg-56), and five uncharged polar residues (Ser-41, Thr-42, Ser-43, Ser-45, and Ser-53). The C-terminal sequence ($_{155}$PERTIPITREE$_{165}$) is unstructured and contains four hydrophobic residues (Pro-155, Ile-159, Pro-160, and Ile-161), two positively charged residues (Arg-157 and Arg-163), three negatively charged residues (Glu-156, Glu-164, and Glu-165), and two uncharged polar residues (Thr-158 and Thr-162). Deleting hydrophobic N-terminal residues 41−58 is expected to reduce chaperone activity toward substrates that are highly unfolded and have a large amount of exposed hydrophobic surface. In contrast, deleting highly polar C-terminal residues 155−165 is expected to affect solubility and the chaperone activity toward substrates that are partially unfolded and have a small amount of exposed hydrophobic surface.

assembly and for the recognition of completely unfolded substrates, while C-terminal residues 155−165 are critical for maintaining the solubility of the chaperone−substrate complex.

EXPERIMENTAL PROCEDURES

Molecular Modeling. The interactive sequences ($_{41}$STSLSPFYLRPPSFLRAP$_{58}$ and $_{155}$PERTIPITREE$_{165}$) were mapped to a three-dimensional (3D) structural model of human αB crystallin. The 3D homology model of human αB crystallin was computed using the X-ray crystal structure of wheat sHSP16.9 as the template as described previously (*9*, *13*, *16*). The Cα root-mean-square deviation between the superimposed model of human αB crystallin and the crystal structure of wheat sHSP16.9 was 3.25 Å.

Mutagenesis, Protein Expression, and Purification. Deletion mutagenesis of human αB crystallin was performed using the QuikChange mutagenesis kit (Stratagene, La Jolla, CA) as described previously (*16*). Primers used to delete residues 41−58 were 5′-GAG TCC AGT GTC AAA CCA GCT Δ CGT CGG GAA AAG ATC AGA CTC CAA CAG-3′ and 5′-CTG TTG GAG TCT GAT CTT TTC CCG ACG Δ AGC TGG TTT GAC ACT GGA CTC-3′. Primers used to delete residues 155−165 were 5′-GGC TGC GGT GAC AGC AGG CTT Δ GCC AGA GAC CTG TTT CCT TGG TCC-3′ and 5′-GGA CCA AGG AAA CAG GTC TCT GGC Δ AAG CCT GCT GTC ACC GCA GCC-3′. Plasmids containing the mutation were sequenced by standard ABI gene sequencing to verify that only desired mutations were introduced. Plasmids containing the verified sequence were transformed into *Escherichia coli* BL21(DE3) cells (Stratagene) for protein expression and purification. Wt αB crystallin and deletion mutants Δ41−58 and Δ155−165 were purified to apparent homogeneity from bacterial lysates using ion exchange and size exclusion chromatography as described previously (*17*). Protein concentrations were determined using the BCA protein assay kit (Pierce, Rockford, IL). Electrospray ionization mass spectrometry and SDS−PAGE densitometric analysis determined that the purified proteins were >97% pure (Figure 2). Proteins were dialyzed into 5 mM PBS (pH 7.0) and stored at −80 °C for further analysis.

Circular Dichroism. The secondary and tertiary structures of wt αB crystallin, Δ41−58, Δ155−165, β_L crystallin, ADH, and CS were evaluated by ultraviolet circular dichroism (UVCD) spectroscopy using a Jasco 720 circular dichroism spectrophotometer at 37 and 50 °C as described previously (*16*). Far-UVCD experiments were performed using samples at a concentration of 0.1 mg/mL in 5 mM PBS (pH 7.0) with a 1 mm path length cuvette. Near-UVCD experiments were performed with samples that were at a concentration of 1.2 mg/mL in 5 mM PBS (pH 7.0) with a 1 mm path length cuvette. Three data sets were collected for each sample at each temperature. The UVCD spectra of the proteins were baseline-corrected using spectra of the buffer [5 mM PBS (pH 7.0)]. Prior to their use in the chaperone assays, the loss of secondary and tertiary structure

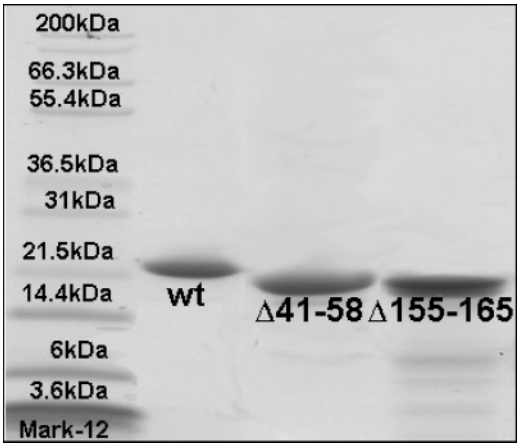

FIGURE 2: SDS−PAGE of purified wt, Δ41−58, and Δ155−165 αB crystallin. Lane 1 contained the molecular mass standard, Mark-12. Lanes 2−4 contained purified wt αB crystallin, Δ41−58, and Δ155−165, respectively. The molecular masses of wt αB crystallin, Δ41−58, and Δ155−165 are 20.2, 18.2, and 18.8 kDa, respectively. All proteins were determined to be >97% pure by densitometric analysis of the SDS−PAGE gel.

of the three substrates was assessed by UVCD spectroscopy: CS ≫ ADH > β_L crystallin (*10*).

Size Exclusion Chromatography. The quaternary structures of wt αB crystallin and the two deletion mutants were determined using an AKTA FPLC purifier (Amersham Biosciences, Piscataway, NJ) and a Superdex 200 HR10/30 column with a molecular mass range of 10−600 kDa (Amersham Biosciences) as described previously (*16*). In three separate runs, 100 μL samples (2.5 mg/mL) were loaded on a pre-equilibrated column and chromatographed at a flow rate of 0.5 mL/min in 5 mM PBS (pH 7.0). The apparent molecular masses of the complex assemblies formed by wt αB crystallin, Δ41−48, and Δ155−165 were calculated from a plot of the elution volume versus log(apparent molecular mass) of calibration proteins. The average number of subunits per complex was calculated from three separate chromatographs using the following formula: number of subunits/complex = apparent molecular mass corresponding to the elution peak/molecular mass of a single wt or mutant αB crystallin subunit.

Chaperone Assays. Chaperone assays of wt αB crystallin, Δ41−58, Δ155−165, $_{41}$STSLSPFYLRPPSFLRAP$_{58}$, and $_{155}$PERTIPITREE$_{165}$ were performed using previously established methods with minor modifications (*16*, *17*). Bovine β_L crystallin (Sigma-Aldrich, St. Louis, MO), equine alcohol dehydrogenase (ADH) (Sigma-Aldrich), and porcine citrate synthase (CS) (Roche, Indianapolis, IN) were used as substrates in the chaperone assays. Chaperone assays were performed in triplicate and at a 1:1 monomeric molar ratio of chaperone to substrate in a 96-well ELISA microtiter plate. For the peptides, chaperone assays at 50:1, 20:1, and 10:1 peptide:substrate concentration ratios were also performed; 0.1 mmol of the chaperone and substrate were mixed in a total volume of 200 μL of buffer [5 mM PBS (pH 7.0)] and heated at 50 °C. The optical density at λ = 340 nm (OD_{340}) was measured using a Multiskan MCC/340 plate reader. Chaperone activity was calculated as the percentage protection in which the maximum light scattering of each substrate protein in the absence of any chaperone was set as 0% protection.

RESULTS

The N-terminal sequence ($_{41}$STSLSPFYLRPPSFLRAP$_{58}$) and the C-terminal sequence ($_{155}$PERTIPITREE$_{165}$) of human αB crystallin were deleted to produce αB crystallin mutants Δ41−58 and Δ155−165, respectively (Figure 1). The deleted N-terminal sequence of residues 41−58 contained 11 hydrophobic residues, two positively charged residues, and five uncharged polar residues. The deleted C-terminal sequence of residues 155−165 contained four hydrophobic, two positively charged, three negatively charged, and two uncharged polar residues. The purity of the proteins was determined to be >97% by SDS−PAGE and densitometric analysis (Figure 2). Mass spectrometry verified the expected decrease in molecular mass of Δ41−58 (to 18.2 kDa) and Δ155−165 (to 18.8 kDa) mutants from 20.2 kDa for wt αB crystallin (data not shown).

The effect of deleting residues 41−58 and 155−165 on the secondary and tertiary structure of αB crystallin was determined by UVCD spectroscopy at 37 and 50 °C (Figure 3). The spectrum of wt αB crystallin exhibited a single broad negative ellipticity minimum between 206 and 218 nm at both temperatures. The far-UVCD spectra of the Δ41−58 and Δ155−165 mutants at both 37 and 50 °C were similar in shape and magnitude to that of wt αB crystallin and contained single broad ellipticity minima between 206 and 218 nm. The secondary structures of wt, Δ41−58, and Δ155−165 αB crystallin were thermostable, and minimal loss of secondary structure was observed when the proteins were heated to 50 °C. The tertiary structures of wt αB crystallin, Δ41−58, and Δ155−165 at 37 and 50 °C were analyzed using near-UVCD spectroscopy (Figure 3). At 37 °C, the spectrum of wt αB crystallin contained four positive molar ellipticity peaks at 259, 270, 284, and 291 nm and a single negative peak at 296 nm corresponding to tryptophan, phenylalanine, and tyrosine residues. The near-UVCD spectra of both Δ41−58 and Δ155−165 at 37 °C exhibited absorption peaks similar to those of wt αB crystallin. The magnitudes of the absorption peaks in the spectra of wt αB crystallin, Δ41−58, and Δ155−165 were temperature-dependent and decreased upon heating at 50 °C. Overall, UVCD analyses of the Δ41−58 and Δ155−165 mutants determined that deleting residues 41−58 and 155−165 had no measurable effect on the structure and thermal stability of αB crystallin.

The effect of deleting residues 41−58 and 155−165 on the complex size of αB crystallin was determined by size exclusion chromatography. The complexes formed by Δ41−58 and Δ155−165 were larger than wt αB crystallin (Figure 4). The chromatograph for wt αB crystallin contained a single peak with an elution volume of 7.7 mL corresponding to a calculated apparent molecular mass of 457 kDa or a complex of 23 subunits. The chromatograph of the Δ41−58 mutant contained two distinct peaks with elution volumes of 6.3 and 7.7 mL corresponding to a calculated apparent molecular mass of 2437 kDa or a complex of 134 subunits and a calculated apparent molecular mass of 420 kDa or a complex of 23 subunits, respectively. The chromatograph of the Δ155−165 mutant contained two major peaks with elution volumes of 7.0 and 7.6 mL and a third minor peak with an elution volume of 11.8 mL corresponding to calculated apparent molecular masses of 1052 kDa or a complex of

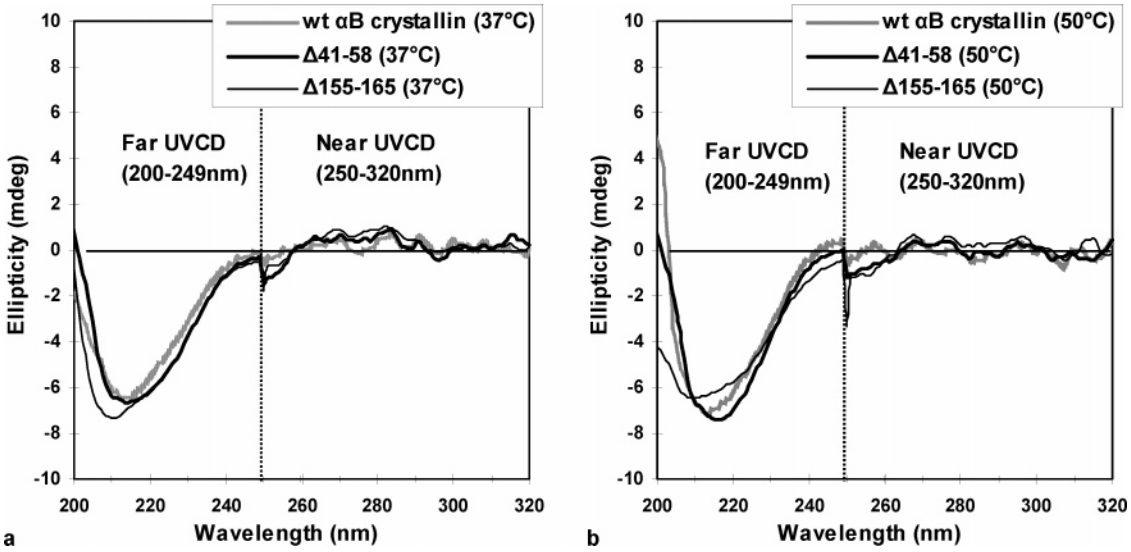

FIGURE 3: Ultraviolet circular dichroism of wt, Δ41−58, and Δ155−165 αB crystallin at 37 (a) and 50 °C (b). The far-UVCD spectra (200−249 nm) of wt, Δ41−58, and Δ155−165 αB crystallin at 37 and 50 °C are similar in shape and magnitude and contained single broad minima between 206 and 218 nm indicating β-sheet−β-turn secondary structure. The near-UVCD spectra (250−320 nm) of wt αB crystallin, Δ41−58, and Δ155−165 at 37 and 50 °C exhibited four positive molar ellipticity peaks at 259, 270, 284, and 291 nm and a single negative peak at 296 nm. On the basis of UVCD spectroscopy, both deletion mutants of αB crystallin appeared to be rich in β-sheet−β-turn secondary structure and were nearly identical to wt αB crystallin.

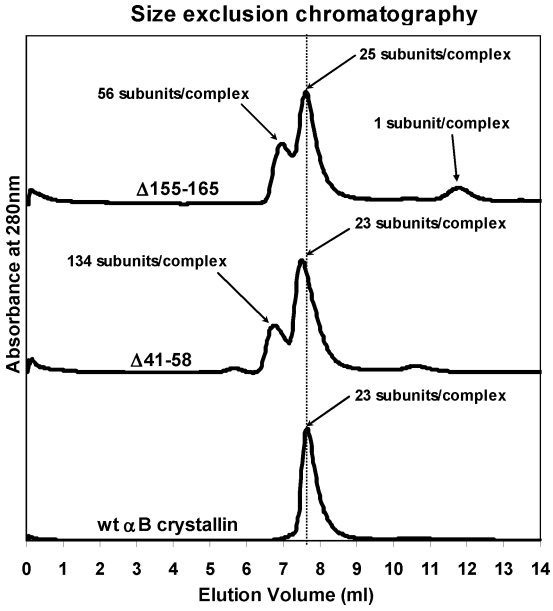

FIGURE 4: Size exclusion chromatography of wt, Δ41−58, and Δ155−165 αB crystallin. Elution profiles of wt αB crystallin, Δ41−58, and Δ155−165 were recorded using a Superdex 200 HR10/30 column. Wt αB crystallin had a single major elution peak at 7.7 mL. The Δ41−58 mutant had two major elution peaks at 6.3 and 7.7 mL. The Δ155−165 mutant had two major elution peaks at 7.0 and 7.6 mL and a minor peak at 11.8 mL. Deletion of the N- and C-terminal interactive sequences altered the size and polydispersity of the αB crystallin complex.

56 subunits, 474 kDa or a complex of 25 subunits, and 25 kDa or a single subunit, respectively. Size exclusion chromatography determined that deletion of residues 41−58 and 155−165 increased the size and polydispersity of the complex formed by αB crystallin.

The chaperone activities of wt, Δ41−58, and Δ155−165 αB crystallin were determined in thermal aggregation assays using 1:1 monomeric molar ratios of three chaperone substrates, β_L crystallin, ADH, and CS (Figure 5). β_L crystallin, a major component of the lens cytoplasm, is a physiological chaperone target, while ADH and CS are model chaperone targets for αB crystallin. Prior to their use in chaperone assays, UVCD spectroscopy determined the unfolding of the three substrate proteins to occur in the following order: CS ≫ ADH > β_L crystallin (*10*). Wt αB crystallin and the deletion mutants were thermostable upon heating at 50 °C for 60 min, and minimal change in optical density at λ = 340 nm (OD_{340}) was observed in the absence of substrate proteins (data not shown). Heating β_L crystallin at 50 °C for 30 min in the absence of a chaperone resulted in limited aggregation of β_L crystallin and an OD_{340} value of 0.03 AU (Figure 5a). Both wt αB crystallin and the Δ41−58 mutant completely inhibited the thermal aggregation of β_L crystallin at 50 °C (Figure 5a). In contrast, the Δ155−165 mutant increased the level of aggregation of β_L crystallin approximately 11-fold. Heating ADH at 50 °C for 30 min in the absence of a chaperone resulted in an OD_{340} of 0.12 AU (Figure 5b). Both wt αB crystallin and the Δ41−58 mutant completely inhibited the thermal aggregation of ADH at 50 °C. In contrast, the Δ155−165 mutant increased the level of aggregation of ADH approximately 3-fold to an OD_{340} value of 0.33 AU. Heating CS at 50 °C for 30 min in the absence of a chaperone resulted in more aggregation than in either β_L crystallin or ADH and corresponded to an OD_{340} value of 0.53 AU (Figure 5c). Wt αB crystallin reduced the level of thermal aggregation of CS at 50 °C by approximately 45%, while the Δ41−58 mutant reduced the level of aggregation of CS at 50 °C by approximately 24%. In contrast to β_L crystallin and ADH, the Δ155−165 mutant had a small protective effect against the thermal aggregation of CS at 50 °C and reduced the level of aggregation of CS by approximately 19%. wt αB crystallin and the Δ41−58 mutant had similar levels of protection, while the Δ155−165 mutant had a reduced level of or no protection with the three substrates. In chaperones assays using synthesized $_{41}$-STSLSPFYLRPPSFLRAP$_{58}$ and $_{155}$PERTIPITREE$_{165}$ pep-

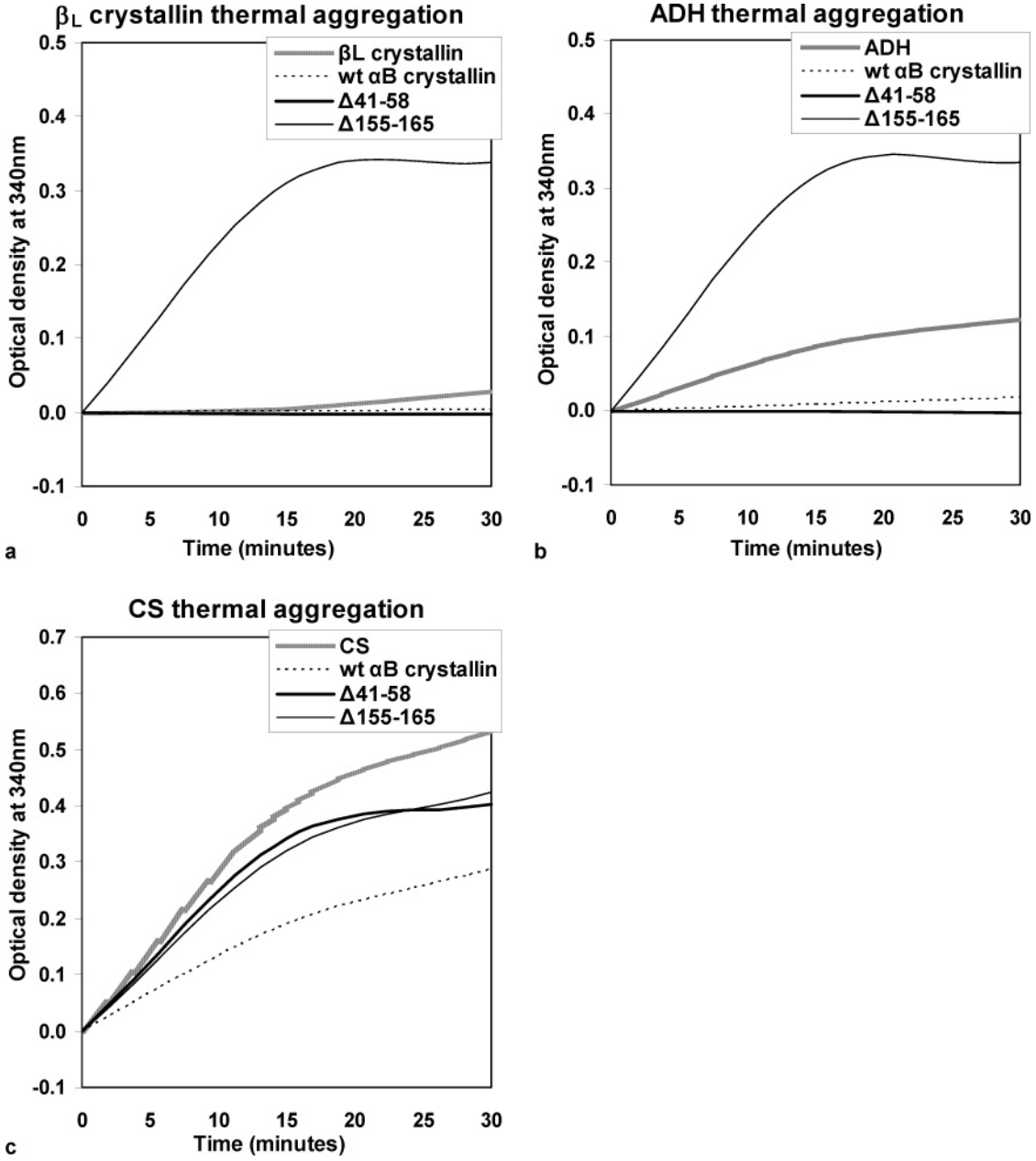

FIGURE 5: Aggregation of β_L crystallin, ADH, and CS in the presence of wt αB crystallin and deletion mutants Δ41−58 and Δ155−165. The effect of wt, Δ41−58, and Δ155−165 αB crystallin on the thermal aggregation of β_L crystallin (a), ADH (b), and CS (c) at a 1:1 monomeric molar ratio was measured using the optical density at $\lambda = 340$ nm (OD_{340}) after samples had been heated at 50 °C for 30 min. The level of aggregation of β_L crystallin decreased from an OD_{340} of 0.03 AU in the absence of chaperone to an OD_{340} of 0.00 AU in the presence of wt αB crystallin and to 0.00 AU in the presence of the Δ41−58 mutant and increased to an OD_{340} of 0.34 AU in the presence of the Δ155−165 mutant. The level of aggregation of ADH decreased from an OD_{340} of 0.12 AU in the absence of chaperone to an OD_{340} of 0.02 AU in the presence of wt αB crystallin and 0.00 AU in the presence of the Δ41−58 mutant and increased to an OD_{340} of 0.33 AU in the presence of the Δ155−165 mutant. The level of aggregation of CS decreased from an OD_{340} of 0.53 AU in the absence of chaperone to 0.29 AU in the presence of wt αB crystallin, 0.40 AU in the presence of the Δ41−58 mutant, and 0.43 AU in the presence of the Δ155−165 mutant. Deleting N-terminal residues 41−58 reduced the chaperone activity toward CS, which was the only completely unfolded substrate, while deleting C-terminal residues 155−165 reduced or abolished chaperone activity for all three substrates (partially and completely unfolded).

tides (data not shown), no protection against aggregation of β_L crystallin, ADH, and CS was observed even at a peptide:substrate concentration ratio as high as 50:1. These results indicated that the αB crystallin sequences ($_{41}$STSLSPFYLRPPSFLRAP$_{58}$ and $_{155}$PERTIPITREE$_{165}$) alone have no chaperone activity.

The Δ41−58 mutant was most effective in protecting the least unfolded substrate (β_L crystallin) and least effective in protecting the most unfolded substrate (CS), indicating that residues 41−58 in αB crystallin were important for recognizing and selecting substrate proteins that were completely unfolded. In contrast, the Δ155−165 mutant had minimal effect on the aggregation of CS and no effect on the aggregation of β_L crystallin and ADH, suggesting that the interactive sequence of residues 155−165 in the C-terminus of αB crystallin was critical for maintaining chaperone−substrate complexes in a soluble state independent of the amount of unfolding of the substrate.

Table 1: Relationship among Unfolding, Aggregation, and Chaperone Activity[a]

substrate	unfolding (ΔΘ)	level of aggregation (AU)			
		no chaperone	+ wt αB Crystallin	+ Δ41−58	+ Δ155−165
β_L crystallin	7%	0.03 ± 0.00	0.00 ± 0.00	0.00 ± 0.00	0.34 ± 0.03
ADH	23%	0.12 ± 0.01	0.02 ± 0.00	0.00 ± 0.00	0.33 ± 0.03
CS	98%	0.53 ± 0.05	0.29 ± 0.01	0.40 ± 0.02	0.43 ± 0.02

[a] Column 1 lists the substrates used in the chaperone assays. Column 2 lists the amount of unfolding of the substrates at 50 °C measured by UVCD spectroscopy and calculated as the change in maximum ellipticity when the substrate was heated from 37 to 50 °C (*10*). Column 3 lists the level of aggregation (OD_{340}) of the substrates in the absence of chaperone after the samples were heated at 50 °C for 60 min. Columns 4−6 list the level of aggregation (OD_{340}) of the substrates in the presence of wt αB crystallin, Δ41−58, and Δ155−165, respectively, after samples were heated at 50 °C for 60 min. Aggregation of the three substrates in the presence of the Δ155−165 mutant appeared to be independent of the amount of substrate unfolding. In the presence of wt αB crystallin and the Δ41−58 mutant, the level of aggregation increased as the amount of substrate unfolding increased.

DISCUSSION

In this report, we demonstrate that deletion of the N-terminal sequence ($_{41}$STSLSPFYLRPPSFLRAP$_{58}$) and the C-terminal sequence ($_{155}$PERTIPITREE$_{165}$) altered the chaperone activity and complex assembly of human αB crystallin. Deleting residues 41−58 and 155−65 altered the size and polydispersity of αB crystallin complexes without having a measurable effect on the secondary and tertiary structure of αB crystallin. In addition to the peak observed at ∼7.7 mL for normal assembly of αB crystallin, the size exclusion chromatographs of the Δ41−58 and the Δ155−165 mutants contained high-molecular mass peaks of 6.3 and 7.0 mL, respectively. The additional peaks may correspond to an alternate arrangement of αB crystallin subunits distinct from the normal arrangement of αB crystallin subunit assemblies. The effect of deleting residues 41−58 and 155−165 from αB crystallin was consistent with the αB crystallin sequences ($_{41}$STSLSPFYLRPPSFLRAP$_{58}$ and $_{155}$PERTIPITREE$_{165}$) being homologous to the wheat sHSP16.9 sequences ($_{20}$PFDTFRSI$_{27}$ and $_{147}$IQI$_{149}$, respectively) that are important for the formation of the dodecameric assembly of wheat sHSP16.9 (*13*). The results confirmed the results of the protein pin arrays which identified the $_{41}$STSLSPFYLRPPSFLRAP$_{58}$ and $_{155}$PERTIPITREE$_{165}$ sequences as interactive sequences for binding both human αA and αB crystallin (*9*). In agreement with previous studies using NMR and truncation mutagenesis (*42*, *43*), deleting residues 155−165 from the C-terminal tail of αB crystallin decreased the solubility and increased the polydispersity of assembled complexes which confirmed the importance of the C-terminal extension domain in the solubility and subunit−subunit interactions of sHSPs.

Wt αB crystallin and the Δ41−58 mutant had similar chaperone activities but different complex sizes, while the Δ41−58 and Δ155−165 mutants had different chaperone activities but similar complex sizes, suggesting that chaperone activity was independent of complex size. The results were consistent with previous studies in which no correlation between complex assembly and chaperone activity was observed for mutants of the β3 and β8 strands of human αB crystallin (*16*, *18*). The decreased chaperone activity of the Δ41−58 and Δ155−165 mutants was consistent with previous protein pin array data in which peptides corresponding to the residues 41−58, 76−82 (β3), 131−138 (β8), 141−144 (β9), and 155−165 had strong interactions with unfolded β/γ crystallin, ADH, and CS (*10*). The effect of deleting residues 41−58 and 155−165 on the chaperone activity of αB crystallin was similar to the effect of mutating residues 76−82 of the β3 strand (*16*), 131−138 of the β8 strand (*18*), and 141−144 of the β9 strand (*17*). While synthesized peptides corresponding to residues 76−82 (β3), 131−138 (β8), and 141−144 (β9) exhibited chaperone activity in vitro (*10*), peptides corresponding to residues 41−58 and 155−165 had no chaperone activity in vitro, suggesting a role in the recognition, selection, and solubility of substrates for N-terminal residues 41−58 and C-terminal residues 155−165. Consistent with this hypothesis, the chaperone activity of the Δ41−58 mutant correlated with the amount of unfolding and aggregation of the three substrates (Table 1). Deleting residues 41−58 had no effect on the chaperone activity for β_L crystallin and ADH which were partially unfolded but decreased the chaperone activity for CS which was completely unfolded. These results indicated that the hydrophobic sequence ($_{41}$STSLSPFYLRPPSFLRAP$_{58}$) was selective for interactions with substrates that were completely unfolded. The Δ155−165 mutant had decreased solubility and reduced or no chaperone activity for any of the three substrates. Even though the substrate β_L crystallin is thermostable and does not form light scattering aggregates when heated at 50 °C, slight unfolding of β_L crystallin was detected at 50 °C by UVCD spectroscopy (*10*). In a previous report, peptides corresponding to C-terminal residues 155−165 of αB crystallin were shown to have stronger interactions with β_L crystallin at 45 °C than with β_L crystallin at 23 °C (*10*). In this report, the optical density of the mixture of β_L crystallin and the Δ155−165 mutant increased when it was heated at 50 °C even though both proteins alone did not aggregate when heated at 50 °C. These results suggested that although the Δ155−165 mutant recognized and bound partially unfolded β_L crystallin, the resultant Δ155−165−β_L crystallin chaperone−substrate complex had low solubility and precipitated out of solution to increase the optical density. These results indicated that C-terminal extension residues 155−165 were critical for the solubility of the chaperone−substrate complexes during chaperone activity independent of the amount of substrate protein unfolding. Together with the results of the mutagenesis of the β3, β8, and β9 strands (*16*−*18*), the results presented here suggest that while the β3−β8−β9 interface on the surface of the α crystallin core domain is important for binding of unfolding substrates, the N-terminal sequence ($_{41}$STSLSPFYLRPPSFLRAP$_{58}$) in αB crystallin recognizes and selects substrates for protection against aggregation on the basis of the amount of substrate protein unfolding, while the $_{155}$PERTIPITREE$_{165}$ sequence

is important for maintaining the solubility of unfolded substrates.

At least five common interactive domains in human αB crystallin participate in the recognition and selection mechanisms used by sHSPs to distinguish between homologous subunits, unfolding substrates, and assembling filament proteins (*9*, *10*). The selective rather than specific nature of the interaction between sHSPs and unfolded substrate proteins appears to be a function of the amount of unfolding and exposed hydrophobic surface of the substrates. The collective response of the five or more interactive domains on sHSPs determines selectivity for similar subunits, unfolding substrate proteins, or filaments in the dynamic equilibrium model for the function of sHSPs in vivo (*22*). Our studies suggest that specific interactive domains on the surface of sHSPs are responsible for the recognition and selection mechanisms of sHSPs for similar subunits, unfolding substrate proteins, or assembling filament proteins. Mutations or post-translational modifications of these interactive domains can shift the dynamic equilibrium to favor complex assembly of sHSP subunits and reduced chaperone activity or dissociation of oligomeric assembly and formation of protective multimeric chaperone−substrate aggregates (*16*, *18*). Continuing investigation of the relative binding affinities of interactive domains in human αB crystallin will characterize the collective interactions used in molecular recognition and selection mechanisms of the sHSPs.

In this report, we characterize the hydrophobic N-terminal sequence ($_{41}$STSLSPFYLRPPSFLRAP$_{58}$) of human αB crystallin as a chaperone sequence involved in the selection and recognition of completely unfolded proteins. Our results indicated that the polar C-terminal sequence ($_{155}$PERTIPITREE$_{165}$) interacted with unfolding proteins to maintain solubility, independent of the amount of substrate protein unfolding.

REFERENCES

1. Sun, Y., and Macrae, T. H. (2005) The small heat shock proteins and their role in human disease, *FEBS Lett. 272*, 2613−27.
2. Arrigo, A. P. (2005) [Heat shock proteins as molecular chaperones], *Med. Sci. (Paris) 21*, 619−25.
3. Laksanalamai, P., and Robb, F. T. (2004) Small heat shock proteins from extremophiles: A review, *Extremophiles 8*, 1−11.
4. Bhattacharyya, J., Udupa, E. G. P., Wang, J., and Sharma, K. K. (2006) Mini-α B-crystallin: A functional element of αB-crystallin with chaperone-like activity, *Biochemistry 45*, 3069−76.
5. Sreelakshmi, Y., and Sharma, K. K. (2005) Recognition Sequence 2 (Residues 60-71) Plays a Role in Oligomerization and Exchange Dynamics of αB-Crystallin, *Biochemistry 44*, 12245−52.
6. Sharma, K. K., Kumar, G. S., Murphy, A. S., and Kester, K. (1998) Identification of 1,1′-bi(4-anilino)naphthalene-5,5′-disulfonic acid binding sequences in α-crystallin, *J. Biol. Chem. 273*, 15474−8.
7. Sun, X., Fontaine, J. M., Rest, J. S., Shelden, E. A., Welsh, M. J., and Benndorf, R. (2004) Interaction of human HSP22 (HSPB8) with other small heat shock proteins, *J. Biol. Chem. 279*, 2394−402.
8. Lentze, N., Studer, S., and Narberhaus, F. (2003) Structural and functional defects caused by point mutations in the α-crystallin domain of a bacterial α-heat shock protein, *J. Mol. Biol. 328*, 927−37.
9. Ghosh, J. G., and Clark, J. I. (2005) Insights into the domains required for dimerization and assembly of human αB crystallin, *Protein Sci. 14*, 684−95.
10. Ghosh, J. G., Estrada, M. R., and Clark, J. I. (2005) Interactive Domains for Chaperone Activity in the Small Heat Shock Protein, Human αB Crystallin, *Biochemistry 44*, 14854−69.
11. Thampi, P., and Abraham, E. C. (2003) Influence of the C-terminal residues on oligomerization of αA-crystallin, *Biochemistry 42*, 11857−63.
12. Van Montfort, R., Slingsby, C., and Vierling, E. (2001) Structure and function of the small heat shock protein/α-crystallin family of molecular chaperones, *Adv. Protein Chem. 59*, 105−56.
13. van Montfort, R. L., Basha, E., Friedrich, K. L., Slingsby, C., and Vierling, E. (2001) Crystal structure and assembly of a eukaryotic small heat shock protein, *Nat. Struct. Biol. 8*, 1025−30.
14. Kim, K. K., Kim, R., and Kim, S. H. (1998) Crystal structure of a small heat-shock protein, *Nature 394*, 595−9.
15. Stamler, R., Kappe, G., Boelens, W., and Slingsby, C. (2005) Wrapping the α-Crystallin Domain Fold in a Chaperone Assembly, *J. Mol. Biol. 353*, 68−79.
16. Ghosh, J. G., Estrada, M. S., and Clark, J. I. (2006) The function of the *β*3 interactive domain in the small heat shock protein and molecular chaperone, human αB crystallin, *Cell Stress Chaperones 11*, 187−97.
17. Muchowski, P. J., Wu, G. J., Liang, J. J., Adman, E. T., and Clark, J. I. (1999) Site-directed mutations within the core "α-crystallin" domain of the small heat-shock protein, human αB-crystallin, decrease molecular chaperone functions, *J. Mol. Biol. 289*, 397−411.
18. Ghosh, J. G., Estrada, M. R., and Clark, J. I. (2006) Structure-Based Analysis of the *β*8 Interactive Sequence of Human αB Crystallin, *Biochemistry 45*, 9878−86.
19. Nicholl, I. D., and Quinlan, R. A. (1994) Chaperone activity of α-crystallins modulates intermediate filament assembly, *EMBO J. 13*, 945−53.
20. Wang, K., and Spector, A. (2001) ATP causes small heat shock proteins to release denatured protein, *Eur. J. Biochem. 268*, 6335−45.
21. Fink, A. L. (1999) Chaperone-mediated protein folding, *Physiol. Rev. 79*, 425−49.
22. Liu, L., Ghosh, J. G., Clark, J. I., and Jiang, S. (2006) Studies of αB crystallin subunit dynamics by surface plasmon resonance, *Anal. Biochem. 350*, 186−95.
23. Shashidharamurthy, R., Koteiche, H. A., Dong, J., and McHaourab, H. S. (2005) Mechanism of chaperone function in small heat shock proteins: Dissociation of the HSP27 oligomer is required for recognition and binding of destabilized T4 lysozyme, *J. Biol. Chem. 280*, 5281−9.
24. Zhang, H., Fu, X., Jiao, W., Zhang, X., Liu, C., and Chang, Z. (2005) The association of small heat shock protein Hsp16.3 with the plasma membrane of *Mycobacterium tuberculosis*: Dissociation of oligomers is a prerequisite, *Biochem. Biophys. Res. Commun. 330*, 1055−61.
25. Chen, X., Fu, X., Ma, Y., and Chang, Z. (2005) Chaperone-like activity of *Mycobacterium tuberculosis* Hsp16.3 does not require its intact (native) structures, *Biochemistry (Moscow) 70*, 913−9.
26. Stromer, T., Fischer, E., Richter, K., Haslbeck, M., and Buchner, J. (2004) Analysis of the regulation of the molecular chaperone Hsp26 by temperature-induced dissociation: The N-terminal domain is important for oligomer assembly and the binding of unfolding proteins, *J. Biol. Chem. 279*, 11222−8.
27. Fu, X., Liu, C., Liu, Y., Feng, X., Gu, L., Chen, X., and Chang, Z. (2003) Small heat shock protein Hsp16.3 modulates its chaperone activity by adjusting the rate of oligomeric dissociation, *Biochem. Biophys. Res. Commun. 310*, 412−20.
28. Srinivas, V., Raman, B., Rao, K. S., Ramakrishna, T., and Rao Ch, M. (2005) Arginine hydrochloride enhances the dynamics of subunit assembly and the chaperone-like activity of α-crystallin, *Mol. Vision 11*, 249−55.
29. Lentze, N., Aquilina, J. A., Lindbauer, M., Robinson, C. V., and Narberhaus, F. (2004) Temperature and concentration-controlled dynamics of rhizobial small heat shock proteins, *Eur. J. Biochem. 271*, 2494−503.
30. Sun, Y., and Macrae, T. H. (2005) Small heat shock proteins: Molecular structure and chaperone function, *Cell. Mol. Life Sci.* (in press).
31. Lentze, N., and Narberhaus, F. (2004) Detection of oligomerisation and substrate recognition sites of small heat shock proteins by peptide arrays, *Biochem. Biophys. Res. Commun. 325*, 401−7.
32. Fu, L., and Liang, J. J. (2002) Detection of protein-protein interactions among lens crystallins in a mammalian two-hybrid system assay, *J. Biol. Chem. 277*, 4255−60.
33. Fu, X., Zhang, H., Zhang, X., Cao, Y., Jiao, W., Liu, C., Song, Y., Abulimiti, A., and Chang, Z. (2005) A dual role for the N-terminal region of *Mycobacterium tuberculosis* Hsp16.3 in self-

oligomerization and binding denaturing substrate proteins, *J. Biol. Chem. 280*, 6337−48.
34. Haslbeck, M., Ignatiou, A., Saibil, H., Helmich, S., Frenzl, E., Stromer, T., and Buchner, J. (2004) A domain in the N-terminal part of Hsp26 is essential for chaperone function and oligomerization, *J. Mol. Biol. 343*, 445−55.
35. Theriault, J. R., Lambert, H., Chavez-Zobel, A. T., Charest, G., Lavigne, P., and Landry, J. (2004) Essential role of the NH_2-terminal WD/EPF motif in the phosphorylation-activated protective function of mammalian Hsp27, *J. Biol. Chem. 279*, 23463−71.
36. Plesofsky, N., and Brambl, R. (2002) Analysis of interactions between domains of a small heat shock protein, Hsp30, of *Neurospora crassa*, *Cell Stress Chaperones 7*, 374−86.
37. Fernando, P., Abdulle, R., Mohindra, A., Guillemette, J. G., and Heikkila, J. J. (2002) Mutation or deletion of the C-terminal tail affects the function and structure of *Xenopus laevis* small heat shock protein, hsp30, *Comp. Biochem. Physiol., Part B: Biochem. Mol. Biol. 133*, 95−103.
38. Studer, S., Obrist, M., Lentze, N., and Narberhaus, F. (2002) A critical motif for oligomerization and chaperone activity of bacterial α-heat shock proteins, *Eur. J. Biochem. 269*, 3578−86.
39. Pasta, S. Y., Raman, B., Ramakrishna, T., and Rao Ch, M. (2004) The IXI/V motif in the C-terminal extension of α-crystallins: Alternative interactions and oligomeric assemblies, *Mol. Vision 10*, 655−62.
40. Saha, S., and Das, K. P. (2004) Relationship between chaperone activity and oligomeric size of recombinant human αA- and αB-crystallin: A tryptic digestion study, *Proteins 57*, 610−7.
41. Carver, J. A., and Lindner, R. A. (1998) NMR spectroscopy of α-crystallin. Insights into the structure, interactions and chaperone action of small heat-shock proteins, *Int. J. Biol. Macromol. 22*, 197−209.
42. Pasta, S. Y., Raman, B., Ramakrishna, T., and Rao Ch, M. (2002) Role of the C-terminal extensions of α-crystallins. Swapping the C-terminal extension of α-crystallin to αB-crystallin results in enhanced chaperone activity, *J. Biol. Chem. 277*, 45821−8.
43. Smulders, R., Carver, J. A., Lindner, R. A., van Boekel, M. A., Bloemendal, H., and de Jong, W. W. (1996) Immobilization of the C-terminal extension of bovine αA-crystallin reduces chaperone-like activity, *J. Biol. Chem. 271*, 29060−6.

BI061471M